

## Immobilization of L-Lysine on Zeolite 4A as an Organic-Inorganic Composite Basic Catalyst for Synthesis of $\alpha,\beta$ -Unsaturated Carbonyl Compounds under Mild Conditions

Farzad Zamani,<sup>†,‡,\*</sup> Mehdi Rezapour,<sup>†,§</sup> and Sahar Kianpour<sup>‡</sup>

<sup>†</sup>Department of Chemistry, Islamic Azad University, Shahreza Branch, Shahreza 31186145, Isfahan, Iran  
\*E-mail: fzamani@iaush.ac.ir

<sup>‡</sup>Central Laboratory Complex, Sheikh-Bahai Department, Isfahan Science and Technology Town, Isfahan University of Technology, Isfahan 8415683111, Iran

<sup>§</sup>Department of Chemistry, Isfahan University of Technology, Isfahan 84156, Iran  
Received February 23, 2013, Accepted May 16, 2013

Lysine (Lys) immobilized on zeolite 4A was prepared by a simple adsorption method. The physical and chemical properties of Lys/zeolite 4A were investigated by X-ray diffraction (XRD), FT-IR, Brunauer-Emmett-Teller (BET), scanning electron microscopy (SEM), transmission electron microscopy (TEM) and UV-vis. The obtained organic-inorganic composite was effectively employed as a heterogeneous basic catalyst for synthesis of  $\alpha,\beta$ -unsaturated carbonyl compounds. No by-product formation, high yields, short reaction times, mild reaction conditions, operational simplicity with reusability of the catalyst are the salient features of the present catalyst.

**Key Words :** Heterogeneous basic catalyst, Lys/zeolite 4A, Organic-inorganic composite, Knoevenagel reaction, Solvent-free condition

### Introduction

$\alpha$ -Amino acids are critical to life because they constitute the building blocks of proteins and biopolymers carrying out the most diverse functions in organisms. The physiological importance of  $\alpha$ -amino acids ensures a sustained interest in their chemistry and properties, particularly in potential applications in many frontiers of modern materials science including biocatalysis,<sup>1-3</sup> drug delivery,<sup>4</sup> and biodegradable plastics industry.<sup>5</sup> In addition, these compounds have received much attention because of their advantages from an environmental as well as a resource standpoint.<sup>6-8</sup>

The immobilization of amino acids and other proteins into inorganic host materials has attracted noticeable attention over the last decade. In terms of catalytic purposes, it is reasonable to assume that immobilization of amino acids on a suitable support is a prerequisite for the use of catalysts in large-scale processing. The development of novel biocatalyst would be in particular useful for the production of pharmaceuticals and fine chemicals. The main challenge is to design functional biocompatible materials and interfacial structures, which allow stable attachment of amino acids while maintaining their activity and function as close as possible to their native state. The adsorption immobilization is proposed to consist of the cationic form of the amino acid attached to the negatively charged inorganic host surface. Moreover, these electrostatic interactions are complemented by hydrophobic interactions probably between neighboring adsorbate molecules.<sup>9</sup> In order to increase the efficiency of amino acid immobilization and catalytic processes, it is

highly desirable to develop materials that have a large surface area, hydrophilic character, high porosity, increased stability with changes in the microenvironment, and high mechanical strength. The adsorption behavior of amino acids on the surfaces of materials such as hydroxyapatite, zirconium phosphate modified silica, silica-gels, activated carbon and zeolite has been investigated.<sup>10-16</sup> Although many cases of successful immobilization using inorganic porous materials have been reported, most of the research published only uses standard activity assays to monitor the catalytic performance. In other words, the application of amino acids adsorbed on inorganic supports in terms of catalytic purposes has received very little attention. Therefore, demonstration of their utility including the possibility to reuse the catalyst is of imminent importance.

Zeolites are the most favorable host materials due to highly ordered pore systems, channels and cages of different dimensions and shapes and the surface with negatively charge-balanced with exchangeable cations.<sup>17,18</sup> Zeolite NaA (4A) is a synthetic zeolite with very small pores. It has a three dimensional pore structure which is composed of sodalite cages, but connected through double four-membered rings (D4R) of  $[\text{SiO}_4]^{4-}$  and  $[\text{AlO}_4]^{5-}$ . The aluminosilicate framework is anionic with large channels of spherical voids. The principal channels have eight-oxygen (sixteen-membered) rings as their minimum constriction. These eight-oxygen rings are shared by the large cavities and allow material to pass to the interior of a zeolite crystal.<sup>19</sup> Due to its low cost and high thermal stability, A-type zeolite has potential applications in separation and catalysis processes.<sup>20</sup>

One of the most favorable interests in organic synthesis, especially in the synthesis of fine chemical products such as pharmaceuticals, is the facile synthesis of new carbon-carbon bonds. Knoevenagel reaction is one of the different types of C-C bond-forming reactions. It is a cross-aldol condensation reaction between a carbonyl group and a methylene-activated substrate for synthesis of  $\alpha,\beta$ -unsaturated compounds. The catalysts traditionally used for this reaction are ammonia, or primary or secondary amines.<sup>21</sup> In recent years, a wide range of catalysts and promoters such as  $\text{NbCl}_5$ ,<sup>22</sup>  $\text{HClO}_4\text{-SiO}_2$ ,<sup>23</sup>  $\text{CeCl}_3\cdot 7\text{H}_2\text{O}/\text{NaI}$ ,<sup>24</sup> zeolites,<sup>25,26</sup>  $\text{TMSCl}$ <sup>27</sup> and ionic liquids<sup>28-30</sup> have been employed to catalyze this reaction in solution or under solvent-free conditions. In spite of the aforementioned efforts for the synthesis of  $\alpha,\beta$ -unsaturated compounds, many of these methods involve expensive reagents, strong acidic/basic conditions, long reaction times, low yields and use of toxic organic solvents, reagents or catalysts. Therefore, to avoid these limitations, the discovery of a new and efficient promoter or catalyst with high catalytic activity, short reaction time, recyclability and simple workup for the preparation of tri-substituted alkenes under mild and practical conditions is of prime interest.

In continuing our study to develop new efficient heterogeneous basic catalysts on inorganic porous materials,<sup>31-33</sup> herein, we will present the heterogenization of lysine on pure zeolite 4A material using a simple adsorption method, which is a simple and eco-environmental friendly organic-inorganic composite basic catalyst for the Knoevenagel condensation of various aldehydes with ethyl cyanoacetate under mild and heterogeneous conditions. To the best of our knowledge, noticeable work as to basic reactions such as Knoevenagel condensation by  $\alpha$ -amino acids adsorbed on inorganic porous materials has not been reported yet.

## Experimental

**Materials.** DL-Lysine monohydrochloride (> 98%, TLC), tetraethyl orthosilicate (TEOS, 98%), tri-block copolymer poly(ethylene glycol)-block-poly(propylene glycol)-block-poly(ethylene glycol) (Pluronic P123, molecular weight = 5800,  $\text{EO}_{20}\text{PO}_{70}\text{EO}_{20}$ ), aluminum tri-*sec*-butylate (97%) and 2,4-pentandione (H-acac) were purchased from Aldrich. Clinoptilolite was obtained from deposits of the Semnan Region, Iran. The sample was ground and only particles smaller than 71  $\mu\text{m}$  (200 mesh) were used for the experiment. Zeolite 4A was provided by Fujian Risheng Chemical. All the reagents used were purchased from Merck in analytical grade quality and further purification was not conducted.

**Catalyst Preparation.** Mesoporous silica SBA-15 through the addition of  $\text{H}_3\text{PO}_4$  was prepared as described in the literature.<sup>34</sup> 2 g of Pluronic P123 were dissolved at room temperature in 4.16 mL of  $\text{H}_3\text{PO}_4$  (85%) and deionized water (75.4 mL), then TEOS (4.6 mL) was added to this solution and the synthesis was carried out by stirring at 35 °C for 24 h in sealed teflon breakers and subsequently placed at

100 °C for 24 h. Then the solution was filtered, washed with deionized water, and finally dried at 95 °C for 12 h in air. Template removal was performed by calcination in air using two successive steps, first heating at 250 °C for 3 h and then at 550 °C for 4 h.

$\text{SiO}_2\text{-Al}_2\text{O}_3$  was also used as the support, which was prepared with the optimized Al/Si molar ratio, described in the previous works.<sup>35</sup> Aluminum tri-*sec*-butylate (97%) and tetraethyl orthosilicate (98%) were used as the precursors, and 2,4-pentandione (H-acac) as the complexing agent. Appropriate amounts of Aluminum tri-*sec*-butylate and tetraethyl orthosilicate were dissolved in the solvent, *n*-butanol. The solution was heated to 60 °C. The components were thoroughly mixed. Then the solution was cooled down to room temperature, and H-acac as the complexing agent was added. This clear solution was hydrolyzed with deionized water (11.0 mol of  $\text{H}_2\text{O}/\text{mol}$  of alkoxide). The solutions were left overnight to hydrolyze the alkoxides, yielding transparent gels. The transparent gels were dried at 110 °C to remove water and solvent, and then calcined at 500 °C for 5 h to remove the organics.

Lysine adsorption on the different adsorbents was carried out according to the procedure previously reported.<sup>36</sup> A series of L-Lysine (Lys) amino acid solutions was prepared by dissolving different amounts of amino acid in deionized water. Afterwards, in each adsorption experiment, 50 mg of the different adsorbents was suspended in 10 mL of the amino acid solution. The pH of the solutions was adjusted prior to mixing using 0.1 M NaOH or 0.1 M HCl. The resulting mixture was continuously shaken in a shaking bath with a speed of 120 rpm at room temperature for 24 h. Finally, the catalyst was separated from the solution by centrifugation. The adsorption amount of amino acid was determined by measuring the change of the amino acid concentration before and after adsorption using UV-vis spectrophotometer at  $\lambda_{\text{max}}$  of lysine, 210 nm. The obtained catalysts were donated as Lys/zeolite 4A, Lys/ $\text{Al}_2\text{O}_3$ , Lys/ $\text{SiO}_2\text{-Al}_2\text{O}_3$  and Lys/SBA-15.

**Apparatus.** The obtained materials were characterized by X-ray diffraction (Bruker D8ADVANCE,  $\text{Cu K}\alpha$  radiation), FT-IR spectroscopy (Nicolet 400D in KBr matrix in the range of 4000-400  $\text{cm}^{-1}$ ), Brunauer-Emmett-Teller (BET) specific surface areas and Barrett-Joyner-Halenda (BJH) pore size distribution (Series BEL SORP 18, at 77 K), scanning electron microscopy (SEM) using Philips XL30 with SE detector, UV-Vis spectroscopy (Varian, Cary 300) and Transmission electron microscopy (TEM) using Phillips CM10 microscope.

**General Procedure for Knoevenagel Condensation Reaction.** In a typical procedure, a mixture of benzaldehyde (2 mmol), ethyl cyanoacetate (2 mmol) and modified Lys/zeolite 4A (0.1 g) was placed in a round bottom flask. The suspension was agitated at room temperature for 10 minutes. Completion of the reaction was monitored by TLC, using *n*-hexane/ethyl acetate (5:1) as eluent. For the reaction workup, the catalyst was removed by filtration and washed with hot ethanol. Then, the solvent was evaporated and a pure

product was obtained. The products were identified using  $^1\text{H-NMR}$ ,  $^{13}\text{C-NMR}$  and FT-IR spectroscopy techniques. Quantitative analyses were conducted with an Agilent 6820 GC equipped by gas chromatography (GC) using a HP 5890 Series II Chromatograph fitted with a packed column (18% Carbowax 20 M/Chromosorb W AW-DMCS), equipped with an HP 5971 Mass Selective Detector.

## Results and Discussion

### Catalyst Characterization.

**XRD:** The XRD patterns of zeolite 4A and Lys/zeolite 4A are presented in Figure 1. Zeolite 4A depicts several sharp characteristic peaks at  $2\theta$  values of  $7^\circ$ ,  $10.4^\circ$ ,  $12.8^\circ$ ,  $16.5^\circ$ ,  $21.6^\circ$ ,  $24^\circ$ ,  $26.2^\circ$ ,  $27^\circ$ ,  $30^\circ$ ,  $31^\circ$ ,  $31.1^\circ$ ,  $32.5^\circ$ ,  $33.5^\circ$  and  $34.3^\circ$  that has been reported in the literature,<sup>37</sup> which can be indexed to the (200), (220), (222), (420), (440), (600), (622), (640), (642), (694), (600), (840), (842) and (664) reflections of the cubic crystalline system and the space group Fm3c.<sup>38</sup> The zeolite 4A and Lys/zeolite 4A samples show the same pattern, indicating that the structure of the zeolite 4A is well retained even after immobilization with lysine. However, the intensity of the characteristic reflection peaks of the Lys/zeolite 4A ( $2\theta = 7-45$ ) sample is found to be reduced (Fig. 1), which is possibly due to the presence of guest moieties onto the framework of zeolite 4A, resulting in the decrease of crystallinity.

**FT-IR:** The FT-IR spectra of zeolite 4A, L-lysine and optimized lysine-supported sample are shown in Figure 2. In the FT-IR spectrum of the zeolite 4A, the characteristic bands for zeolite framework at  $565\text{ cm}^{-1}$  due to the external vibration of double four-rings,  $1010\text{ cm}^{-1}$  for the internal vibration of (Si, Al)-O asymmetric stretching,  $688\text{ cm}^{-1}$  for the internal vibration of (Si, Al)-O symmetric stretching, and  $470\text{ cm}^{-1}$  for the internal vibration of (Si, Al)-O bending were observed (Fig. 2(a)). The broad band at around  $3100-$

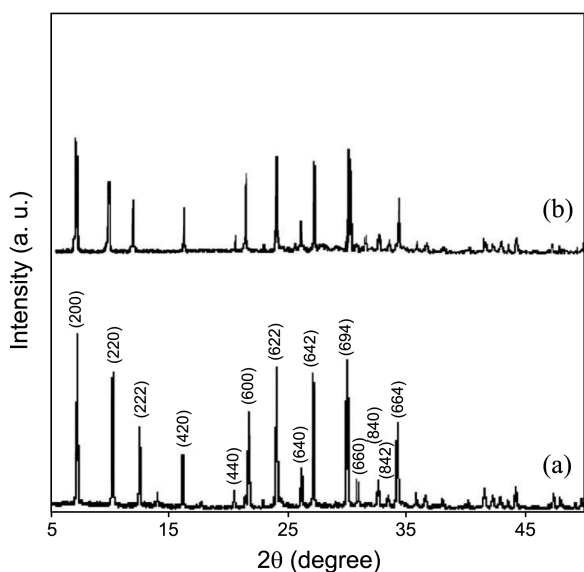


**Figure 1.** The powder XRD pattern of (a) zeolite 4A and (b) Lys/zeolite 4A.

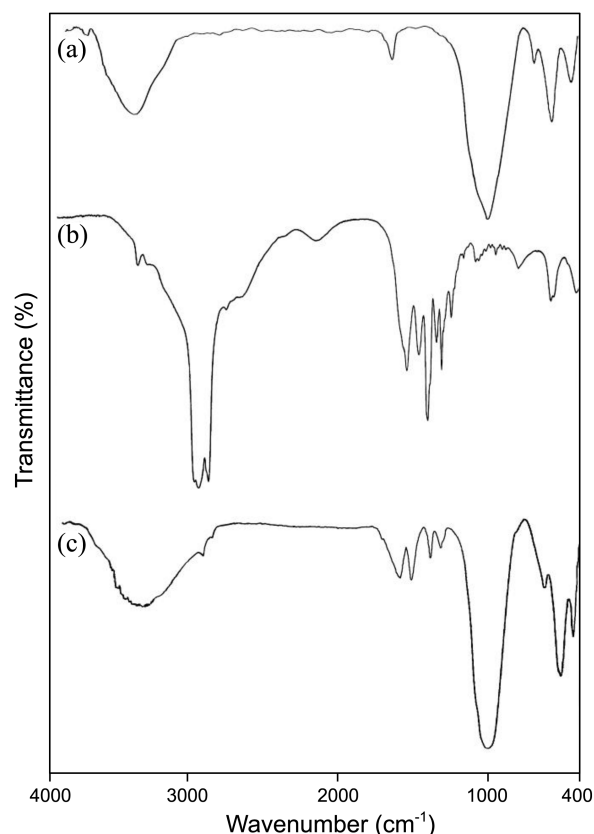


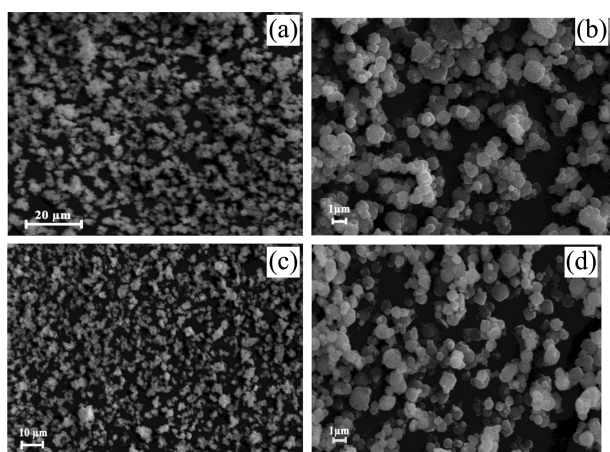
**Figure 2.** FT-IR spectra of (a) zeolite 4A, (b) lysine and (c) Lys/zeolite 4A.

$3600\text{ cm}^{-1}$  and the sharp one at  $1665\text{ cm}^{-1}$ , which are related to OH, also appeared.<sup>39-42</sup> In terms of Lys/zeolite 4A, the presence of peaks at about  $2900\text{ cm}^{-1}$  is attributed to the aliphatic C-H stretching of the amino acid, which is at low intensity because of the very broad band of zeolite (Fig. 2(c)). These are in accordance with the spectrum of Lys (Fig. 2(b)). The bands at  $1418\text{ cm}^{-1}$ ,  $1595\text{ cm}^{-1}$  and  $1519\text{ cm}^{-1}$ , and are respectively assigned to  $\text{COO}^-_{\text{as}}$ ,  $\text{COO}^-_{\text{as}}$  plus  $\text{NH}^{+3}_{\text{sd}}$  ( $\alpha$ -amino group) and  $\text{NH}^{+3}_{\text{sd}}$  (side-chain amino group).<sup>43</sup> Furthermore, the FT-IR spectrum of Lys/zeolite 4A has no an absorption band at  $1733\text{ cm}^{-1}$  ( $\text{C=O}_{\text{as}}$ ) which indicates that the  $\alpha$ -carboxyl group is completely present in the deprotonated form ( $\text{COO}^-$ ) (Fig. 2(c)). Hence, the FT-IR spectroscopic analysis exhibits that the major fraction of lysine adsorbed onto the silica surface is in the cationic state.<sup>43</sup> Kitadai has reported that if lysine adsorbs on montmorillonite through the  $\alpha$ -amino group, both of the characteristic bands of  $\alpha$ -amino group and side-chain amino group are likely shift to lower wavenumbers,<sup>44</sup> which similarly did not occur in Lys/zeolite 4A. Therefore, it might be deduced that lysine adsorbed on zeolite 4A through the protonated side-chain amino group but not through the protonated  $\alpha$ -amino group.

**$\text{N}_2$  Adsorption-Desorption Isotherms.** The specific surface area and the pore size of the samples are summarized in Table 1. It can be seen that the pore volume and the surface area of zeolite 4A decreased drastically after Lys adsorption

**Table 1.** Physical properties of the samples

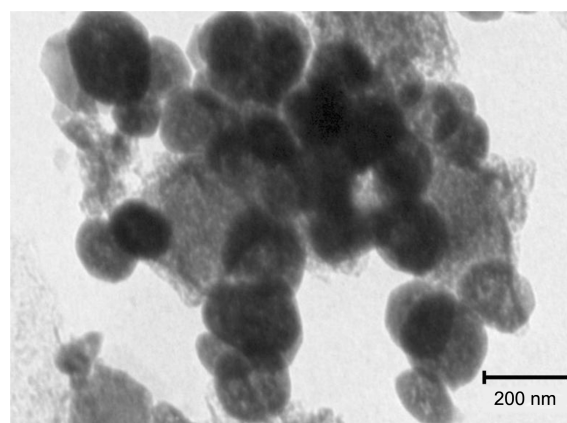
Sample	BET surface area (m <sup>2</sup> g <sup>-1</sup> )	Pore volume (cm <sup>3</sup> g <sup>-1</sup> )	Average pore diameter (nm)
SBA-15	1400	1.90	9
Clinoptilolite	20.8	0.03	0.61
Zeolite 4A	210.4	0.22	0.73
Al <sub>2</sub> O <sub>3</sub>	330	0.25	5
SiO <sub>2</sub> -Al <sub>2</sub> O <sub>3</sub>	498	0.46	4.5
Lys/Zeolite 4A	113.7	0.17	0.95

**Figure 3.** Scanning electron microscopy (SEM) photographs of (a,b) zeolite 4A and (c,d) Lys/zeolite 4A.

from 210.4 to 113.7 m<sup>2</sup> g<sup>-1</sup> and 0.22 to 0.17 cm<sup>3</sup> g<sup>-1</sup> respectively. This large reduction in the specific pore volume and the specific surface area could be attributed to the tight packing of Lys molecule inside the pore channels of zeolite 4A. On the other hand, the data for the Lys/SiO<sub>2</sub>-Al<sub>2</sub>O<sub>3</sub> and Lys/zeolite 4A samples indicated a growth in the average pore diameter in comparison to Al<sub>2</sub>O<sub>3</sub>-SiO<sub>2</sub> and zeolite 4A. The results are likely attributed to the presence of lysine in the structure of catalyst.

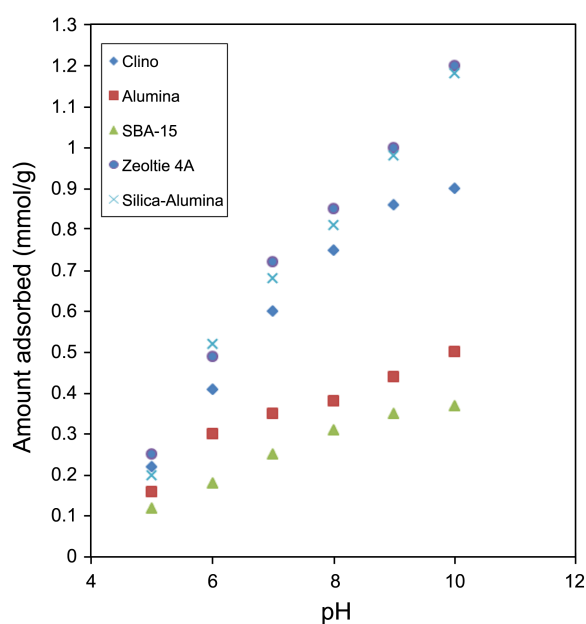
**SEM:** Figure 3 shows the SEM images of the zeolite 4A and Lys/zeolite 4A samples. These figures reveal that Lys/zeolite 4A (Fig. 3(c), (d)) has approximately the same morphology as commonly observed in zeolite 4A (Fig. 3(a), (b)), which can be described as truncated-side cubic crystals with a size in the range 1-2 μm. This finding indicates that there is no change in the morphology of silica after being modified with the amino acid. As a result, N<sub>2</sub> adsorption and SEM image of the samples after lysine adsorption reveal that the amino acid molecule is packed inside the pore channels of zeolite 4A adsorbent.

**TEM:** The TEM micrograph of Lys/zeolite 4A is depicted in Figure 4. It can be seen that the sample has uniform particle size of about 100-200 nm, and the places with darker contrast could be assigned to the presence of lysine with different dispersion, probably located into the support pores, which is in accordance with the SEM images, BET and XRD results.

**Figure 4.** Transmission electron microscopy (TEM) image of Lys/zeolite 4A.

**Effect of Operational Parameters on the Lysine Adsorption.** The adsorption of lysine has been studied under a range of solution conditions, *e.g.*, pH, amino acid concentration, contact time and different supports, to reach an optimum condition.

In order to find out the adsorption capacity of adsorbents, the Lys adsorption isotherms of five different adsorbent materials, *i.e.* clinoptilolite, Al<sub>2</sub>O<sub>3</sub>, SiO<sub>2</sub>-Al<sub>2</sub>O<sub>3</sub>, zeolite 4A and SBA-15, have been determined at different buffer solution pH ranging from 5 to 10 (Fig. 5). In general, there are four different dissociation states of lysine in an aqueous media, including di-cationic, cationic, zwitterionic, and anionic, which are mainly dependent on solution pH.<sup>45</sup> It means that as pH increases, the dissociation state changes from di-cationic to anionic form. Near the isoelectric point of lysine (9.7), although the zwitterionic state is the major dissociation state of dissolved lysine, it has been revealed that the

**Figure 5.** Lysine adsorption isotherms on various porous adsorbents at different pH conditions (concentration of lysine = 10 mmol L<sup>-1</sup>, 24 h, room temperature).

major fraction of lysine adsorbed onto the adsorbent surface is in the cationic state.<sup>43,44</sup> It can be seen that there is an upward trend in the amount of Lys adsorbed onto all the adsorbents over the pH range of 5 to nearly 10, reaching a point of maximum lysine adsorption at pH 10, which is close to the isoelectric point of lysine (9.7). It has been shown in some studies that proteins tend to adsorb onto surfaces more via strong electrostatic interactions between the surface and the protein.<sup>46</sup> In the pH range of 5 to nearly 10, the amount of adsorbed cationic lysine swiftly increases because the surface becomes more negatively charged, whereas the mole fraction of cationic lysine in the solution do not substantially change. As a result, the adsorption could be mainly driven by the strong electrostatic interaction between the negatively charged zeolite 4A surface and the positively charged cationic lysine. Although the mole fraction of cationic lysine in the solution decreases at high pH, the amount of adsorbed cationic lysine still increases slowly. It can be explained that the surface charge density of the negatively charged surface increases faster than the mole fraction of cationic lysine decreased in solution.<sup>47</sup>

It is also obvious from Figure 5 that the adsorption capacities of the different adsorbents have the following order: zeolite 4A > SiO<sub>2</sub>-Al<sub>2</sub>O<sub>3</sub> > clinoptilolite > Al<sub>2</sub>O<sub>3</sub> > SBA-15, although SBA-15 has higher surface areas as compared to the other adsorbents (Table 1). In the case of zeolite 4A, the presence of well-ordered pore system supports the diffusion of the Lys molecule into the interior part of the pores. Moreover, the surface area of zeolite 4A is higher than the clinoptilolite and provides the way for more accessible adsorption sites. Therefore, the adsorption capacity of zeolite 4A is higher than clinoptilolite. By contrast, although SBA-15 has a higher mesopore volume and ultra large pore diameter, the Lys adsorption capacity is quite low. This indicates that in terms of SBA-15, the surface characteristic of the adsorbent plays an important role in determining the adsorption capacity. It has been previously reported that the surface hydroxyl groups of SBA-15 is around 4.1 OH groups per nm<sup>2</sup>.<sup>48</sup> These surface hydroxyl groups may prefer to form hydrogen bond with the water molecules present in the buffer rather than the Lys molecules and form a hydration sphere on the surface. This would suppress the interaction between the Lys molecule and the adsorbent surface. Therefore, the reduction in the adsorption capacity is expected. Moreover, it is well known fact that the pore curvature decreases with increasing pore diameter. The reduced pore curvature also affects the interaction between the neighbouring lysine molecules which reduces the tight packing of the lysine molecules.<sup>14</sup> As can be seen, SBA-15 has the highest pore diameter in comparison to the other supports. As a result, although SBA-15 has the high acidic site and pore volume, the low Lys adsorption capacity is expected due to these aspects. In addition, According to the data, it can be said that pore size do not affect the adsorption of lysine on zeolites, which is in agreement with the previous works.<sup>36,49</sup> Moreover, as lysine amino acid is hydrophilic, the hydrophilicity/hydrophobicity of zeolitic materials, which

is affected by their Si/Al ratio, plays a key role in the adsorption of amino acids onto the zeolite surface.<sup>49,50</sup> It is assumed that zeolites with high Si/Al ratio show hydrophobic character.<sup>49</sup> Compared with SBA-15, zeolite 4A and SiO<sub>2</sub>-Al<sub>2</sub>O<sub>3</sub> are rich in alumina, which leads to having hydrophilic surface. As a result, the adsorption of lysine on these zeolites is higher than SBA-15 due to the hydrophilicity. In addition, in terms of zeolite 4A, the electrical imbalance arising from the substitution of Si<sup>4+</sup> by Al<sup>3+</sup> in the structure of zeolites is compensated by balancing cations held electrostatically within the zeolite. These cations are not an integral part of the zeolite Si/Al-O framework and are usually called exchangeable cations, since they are fairly mobile and readily replaced by other cations. Therefore, these exchangeable cations might improve the amino acid adsorption capacity of zeolite 4A.

As a result, from the industrial point of view, since zeolite 4A is easily available among the solid-acid catalysts, it was employed for the further steps.

In order to test the influence of amino acid concentration, Lys adsorption was determined at six different amino acid concentrations, ranging from 5 to 30 mmol L<sup>-1</sup> at the pH 10 (Fig. 6). The amount of amino acid adsorption onto zeolite 4A significantly increased with raising initial concentration of amino acid solution. This phenomenon can be explained that when the amino acid concentration in the bulk is low, the amino acid is randomly deposited on the adsorbent surface. On the contrary, when the amino acid concentration is high, functional group of the two or more amino acid side chains approaches each other until they touch within their van der Waals radii, and helps close packing of the amino acid molecules.<sup>51,52</sup> According to the results, 25 mmol L<sup>-1</sup> was selected as the optimized Lys adsorption, which exhibited the total adsorption of 2.65 mmol g<sup>-1</sup> on the zeolite 4A surface.

The time dependence of lysine adsorption onto zeolite 4A was investigated to determine the time required for equilibrium to be reached between the solid and solution (Fig. 7).

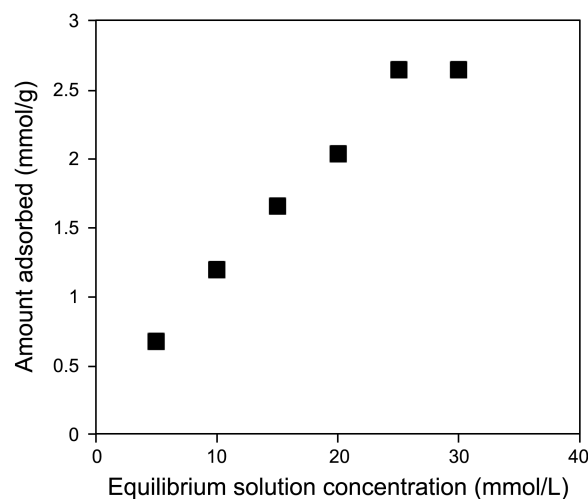


**Figure 6.** Adsorption isotherm for lysine onto zeolite 4A (pH = 10, 24 h, room temperature).

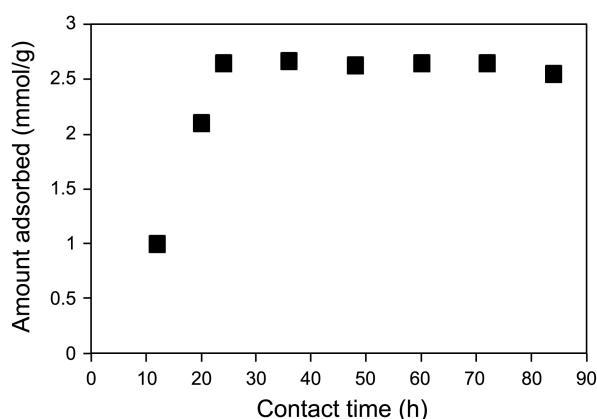


**Figure 7.** Contact time (lysine concentration = 25 mmol g<sup>-1</sup>, pH = 10, room temperature).

It is clear from the figure that the adsorbed amount increases with contact time to reach a plateau of 2.65 mmol g<sup>-1</sup> at 24 h. Looking more closely at the trend for the lysine adsorption, it can be seen that a slow reduction in adsorbed amount begins from 72 h onwards, which could be attributed to a loss of stability in the zeolite 4A. In other words, the porous structure of zeolite 4A is likely degraded upon extended exposure to water.

**Adsorption Behavior of Lysine on Zeolite 4A.** In general, there are three types of surface hydroxyl groups in the structure of zeolite 4A including Al-OH, Si-OH and Si-OH-Al. The Brønsted acidity of the three hydroxyl protons increases in the order Si-OH-Al > Al-OH > Si-OH, with the bridging hydroxyl proton being the strongest acid.<sup>53-56</sup> Therefore, the basic media interacts with the bridging hydroxyl protons more than the other protons and the surface of zeolite 4A becomes more negatively charged. Hence, the adsorption behavior can be explained by the electrostatic interaction between the negatively charged surface and the positively charged lysine. Another possibility increases in the contribution of hydrophobic interaction between the side-chain alkyl groups of neighboring adsorbing lysine with increasing pH and amino acid concentration.<sup>57,58</sup> As the amount of adsorbed lysine increases, each adsorbed lysine molecule approaches more closely together, and the adsorbate-adsorbate interaction becomes stronger. As a result, the hydrophobic interaction would complement the electrostatic interaction between lysine and zeolite 4A surface. Hence, it might be expected that lysine has a strong adsorption on the zeolite 4A surface which would be suitable for catalytic purposes.

**Effect of Reaction Parameters on the Catalytic Activity.** The Knoevenagel condensation of benzaldehyde with ethyl cyanoacetate was chosen as a model reaction to test the catalytic activity of the Lys/zeolite 4A. Therefore, the effect of various reaction parameters on the condensation of benzaldehyde with ethyl cyanoacetate has been studied using Lys/zeolite 4A as a basic catalyst.

Different solvents such as water, acetonitrile, methanol and dichloromethane were used for the Knoevenagel con-

**Table 2.** Effect of solvent on the Knoevenagel condensation over Lys/zeolite 4A<sup>a</sup>

Solvent	Yield (%) <sup>b</sup>
Methanol	58
Dichloromethane	75
Water	60
Acetonitrile	67
Solvent-free	83

<sup>a</sup>Reaction conditions: catalyst (0.06 g), benzaldehyde (2 mmol), ethyl cyanoacetate (2 mmol), room temperature, reaction time = 10 min, selectivity = 100%. <sup>b</sup>Isolated yield

densation over Lys/zeolite 4A. The solvent-free condition was studied as well. The results are summarized in Table 2. As mentioned earlier, according to the FT-IR spectroscopic analysis, the major fraction of lysine adsorbed onto the silica surface is in the cationic state. Hence, it could be expected that the surface of the catalyst consists of both basic and acid sites (NH<sub>3</sub><sup>+</sup> and COO). It can be seen that the highest yield of 83% was obtained in the absence of solvent. Although the reactants, intermediates and products are more stabilized in polar solvents such as water,<sup>59</sup> the catalyst showed a lower activity in water compared with the solvent-free condition. A reasonable explanation is that the amino acid adsorbed on zeolite 4A can be flushed with water, which leads to pore blocking as well as reducing the active sites of the catalyst. It is also expected that the acid and base groups in Lys/zeolite 4A would be in equilibrium between the free acid-base and the ion pair, which results from neutralization. Therefore, the solvent could have a dramatic effect on this equilibrium. In general, protic solvents would confer different properties to aprotic solvents as a result of differing abilities to stabilize the neutralized ion pair. The equilibrium would lie towards the ion pair in protic solvents, *e.g.* methanol and water, as proton exchange would be rapid and the protic solvent would stabilize the ion pair the most. Aprotic solvents such as dichloromethane and acetonitrile would cause slower exchange of the protons and would stabilize the ion pair much less than a protic solvent, forcing the equilibrium in favor of the free acid and base.<sup>60</sup>

In order to investigate the importance of amount of the catalyst, the Knoevenagel reaction between benzaldehyde and ethyl cyanoacetate over Lys/zeolite 4A was investigated

**Table 3.** Effect of amount of catalyst on the Knoevenagel condensation over Lys/zeolite 4A<sup>a</sup>

Catalyst amount (g)	Yield (%) <sup>b</sup>
0.02	55
0.04	75
0.06	83
0.1	98
0.12	98

<sup>a</sup>Reaction conditions: benzaldehyde (2 mmol), ethyl cyanoacetate (2 mmol), solvent-free, room temperature, reaction time = 10 min, selectivity = 100%. <sup>b</sup>Isolated yield

**Table 4.** Recyclability of the catalyst<sup>a</sup>

Reaction cycles	Yield (%) <sup>b</sup>
Fresh	98
1	96
2	93
3	90
4	88

<sup>a</sup>Reaction conditions: benzaldehyde (2 mmol), ethyl cyanoacetate (2 mmol), solvent-free, room temperature, reaction time = 10 min, selectivity = 100%. <sup>b</sup>Isolated yield

by different amounts of the catalyst (Table 3). It is observed that while the amount of *Lys*/zeolite 4A increases from 0.02 to 0.1 g, the product yield rises significantly from 55% to 98%. It is because of the availability of more acid-base sites, which favors the dispersion of more active species. Afterwards, the percentage of yield remains stable at 98% between 0.1 g and 0.12 g.

In order to investigate effect of the support (zeolite 4A) on the Knoevenagel reaction, lysine (with the same ratio of the optimized catalyst) without any support as catalyst was used in the Knoevenagel reaction of benzaldehyde by keeping other parameters constant. After 24 h, approximately 75% yield was observed. Therefore, the adsorption of lysine onto the zeolite 4A (as a support) is a valuable way to improve the catalytic activity of the amino acid for the Knoevenagel reaction.

In the view of green chemistry, the reusability of the catalyst was also studied by using *Lys*/zeolite 4A in recycling experiments (Table 4). In order to regenerate the catalyst, after completion of the reaction, it was separated by centrifuge and washed several times with deionized water. Then, it was dried at 60 °C and reused in the subsequent run. By using regenerated sample after four cycles, the yield decreased by 10% and the selectivity was constant (100%).

**Application of *Lys*/zeolite 4A in Knoevenagel Condensation of Various Aldehydes with Ethyl Cyanoacetate.** Our major concern was to examine the activity and selectivity of prepared catalyst for basic reactions such as Knoevenagel condensation. Accordingly, a number of Knoevenagel condensation reactions were carried out with a variety of aromatic and aliphatic aldehydes with ethyl cyanoacetate over *Lys*/zeolite 4A, after ascertaining the optimum experimental conditions. The results are represented in Table 5. It is notable that the aromatic aldehydes, having different substituents such as chloro, nitro, methoxy and methyl, were converted to the corresponding arylidene derivatives with good to high yields. The aromatic aldehydes with electron-withdrawing groups such as chloro and nitro proceeded at faster rates than those with electron-donating groups such as methoxy and methyl. These results showed that electron-donating substituents in aromatic ring appear to retard the rate of reaction due to inactivation of aldehyde group. In addition, the Knoevenagel condensation was carried out using aliphatic aldehydes, which represented the high product yields. Interestingly, the results clearly established that

**Table 5.** Knoevenagel condensation reaction of various aromatic and aliphatic aldehydes and ethyl cyanoacetate catalyzed by *Lys*/zeolite 4A<sup>a</sup>

Entry	Substrate	Product	Time (min)	Yield (%) <sup>b</sup>
1			10	98
2			40	98
3			40	98
4			10	80
5			5	95
6			5	95
7			5	98
8			30	90
9			35	95
10			20	90

<sup>a</sup>Reaction conditions: catalyst (0.1 g), ethyl cyanoacetate (2 mmol), substrate (2 mmol), solvent-free condition, room temperature, selectivity = 100%. <sup>b</sup>Isolated yield

the obtained products were E-isomer forms.

## Conclusion

In conclusion, our studies showed that the immobilization of lysine amino acid onto zeolite 4A serve as highly active organic-inorganic composite basic catalyst for the Knoevenagel reaction of various aromatic and aliphatic aldehydes with ethyl cyanoacetate. The merit of this methodology is that it is simple, fast, mild, and efficient. Therefore, we believe that the reported catalyst could greatly contribute to the environmentally greener and safer process.

**Acknowledgments.** Dr. C. Hyland (University of Wollongong) is gratefully acknowledged for his helpful comments. The authors also thank the Isfahan Science and Technology Town for the support of this work. And the publication cost of this paper was supported by the Korean Chemical Society.

## References

- Dalko, P. I.; Moisan, L. *Angew. Chem. Int. Ed.* 2001, 40, 3726.

2. Jarvo, E. R.; Miller, S. J. *Tetrahedron* **2002**, *58*, 2481.
3. Erkkila, A.; Majander, I.; Pihko, P. M. *Chem. Rev.* **2007**, *107*, 5416.
4. Bourke, S. L.; Kohn, J. *Adv. Drug Delivery Rev.* **2003**, *55*, 447.
5. Sanda, F.; Endo, T. *Macromol. Chem. Phys.* **1999**, *200*, 2651.
6. Ma, J. A. *Angew. Chem. Int. Ed.* **2003**, *42*, 4290.
7. Maruoka, K.; Ooi, T. *Chem. Rev.* **2003**, *103*, 3013.
8. Plaquevent, J. C.; Levillain, J.; Guillen, F.; Malhiac, C.; Gaumont, A. C. *Chem. Rev.* **2008**, *108*, 5035.
9. Ernst, S.; Hartmann, M.; Munsch, S. *Stud. Surf. Sci. Catal.* **2001**, *135*, 308.
10. Palit, D.; Moulik, S. P. *J. Colloid Interf. Sci.* **2001**, *239*, 20.
11. El Shafei, G. M. S.; Moussa, N. A. *J. Colloid Interf. Sci.* **2001**, *238*, 160.
12. El Shafei, G. M. S. *J. Colloid Interf. Sci.* **2002**, *250*, 394.
13. Munsch, S.; Hartmann, M.; Ernst, S. *Chem. Commun.* **2001**, 1978.
14. Vinu, A.; Hossain, K. Z.; Kumar, G. S.; Ariga, K. *Carbon* **2006**, *44*, 530.
15. Casado, C.; Castán, J.; Gracia, I.; Yús, M.; Mayoral, A.; Sebastián, V.; López-Ram-de-Viu, P.; Uriel, S.; Coronas, J. *Langmuir* **2012**, *28*, 6638.
16. Krohn, J. E.; Tsapatsis, M. *Langmuir* **2005**, *21*, 8743.
17. Yamada, M.; Yano, J.; Nakaoka, K.; Ogura, K. *Synth. Met.* **2003**, *138*, 419.
18. Barrer, R. M. *Zeolites and Clay Minerals as Sorbents and Molecular Sieves*; Academic Press: London, UK, 1978.
19. Vanagida, R. Y.; Amaro, A. A.; Seff, K. J. *J. Phys. Chem.* **1973**, *77*, 906.
20. Yang, H.; Chen, H.; Du, H.; Hawkins, R.; Craig, F.; Ring, Z.; Omotoso, O.; Munoz, V.; Mikula, R. *Micropor. Mesopor. Mater.* **2009**, *117*, 33.
21. Jones, G. *Organic Reactions* **1967**, *15*, 204.
22. Yadav, J. S.; Bhunia, D. C.; Singh, V. K.; Srihari, P. *Tetrahedron Lett.* **2009**, *50*, 2470.
23. Kantevari, S.; Bantu, R.; Nagarapu, L. *J. Mol. Catal. A: Chem.* **2007**, *269*, 53.
24. Bartoli, G.; Beleggia, R.; Giuli, S.; Giuliani, A.; Marcantoni, E.; Massacesi, M.; Paletti, M. *Tetrahedron Lett.* **2006**, *47*, 6501.
25. Saravanamurugan, S.; Palanichamy, M.; Hartmann, M.; Murugesan, V. *Appl. Catal. A* **2006**, *298*, 8.
26. Gracia, M. D.; Jurado, M. J.; Luque, R.; Campelo, J. M.; Luna, D.; Marinas, J. M.; Romero, A. A. *Micropor. Mesopor. Mater.* **2009**, *118*, 87.
27. Ryabukhin, S. V.; Plaskon, A. S.; Volochnyuk, D. M.; Pipko, S. E.; Shivanyuk, A. N.; Tolmachev, A. A. *J. Comb. Chem.* **2007**, *9*, 1073.
28. Wang, Y.; Shang, Z. C.; Wu, T. X.; Fan, J. C.; Chen, X. *J. Mol. Catal. A: Chem.* **2006**, *253*, 212.
29. Ranu, B. C.; Jana, R. *Eur. J. Org. Chem.* **2006**, *16*, 3767.
30. Forbes, D. C.; Law, A. M.; Morrison, D. W. *Tetrahedron Lett.* **2006**, *47*, 1699.
31. Abbaspourrad, A.; Kalbasi, R. J.; Zamani, F. *Chin. J. Chem.* **2010**, *28*, 2074.
32. Kolahdoozan, M.; Kalbasi, R. J.; Shahzeidi, Z. S.; Zamani, F. *J. Chem.* **2013**, *2013*, doi:10.1155/2013/496837.
33. Kalbasi, R. J.; Shahzeidi, Z. S.; Zamani, F. *Iranian J. Catal.* **2011**, *1*, 55.
34. Colilla, M.; Balas, F.; Manzano, M.; Vallet-Regí, M. *Chem. Mater.* **2007**, *19*, 3099.
35. Ghiaci, M.; Rezaei, B.; Kalbasi, R. J. *Talanta* **2007**, *73*, 37.
36. O'Connor, A. J.; Hokura, A.; Kisler, J. M.; Shimazu, S.; Stevens, G. W.; Komatsu, Y. *Sep. Purif. Techn.* **2006**, *48*, 197.
37. Treacy, M. J.; Higgins, J. B. *Collection of Simulated XRD Powder Patterns for Zeolites*; Elsevier: Amsterdam, The Netherlands, 2001; p 379.
38. Gramlich, V.; Meier, W. M. Z. *Kristallogr. Kristallgeom. Kristallphys. Kristallchem.* **1971**, *133*, 134.
39. Stevens, R. W.; Siriwardane, R. V.; Logan, J. *Energy Fuels* **2008**, *22*, 3070.
40. Yamada, H.; Yokoyama, S.; Watanabe, Y.; Uno, H.; Tamura, K. *Sci. Technol. Adv. Mater.* **2005**, *6*, 394.
41. Huang, Y.; Jiang, Z. *Micropor. Mater.* **1997**, *12*, 341.
42. Iyer, K. A.; Singer, S. J. *J. Phys. Chem.* **1994**, *98*, 12679.
43. Kitadai, N.; Yokoyama, T.; Nakashima, S. *J. Colloid Interface Sci.* **2009**, *329*, 31.
44. Kitadai, N.; Yokoyama, T.; Nakashima, S. *J. Colloid Interface Sci.* **2009**, *338*, 395.
45. Humblot, V.; Methivier, C.; Pradier, C. M. *Langmuir* **2006**, *22*, 3089.
46. Hartmann, M. *Chem. Mater.* **2005**, *17*, 4577.
47. Goyne, K. W.; Zimmerman, A. R.; Newalkar, B. L.; Komarneni, S.; Brantley, S. L.; Chorover, J. J. *Porous Mater.* **2002**, *9*, 243.
48. Munsch, S. *Adsorption of Amino Acids Over Micro and Mesoporous Molecular Sieves*; Ph.D. thesis, Kaiserslautern University of Technology, 2003.
49. Carneiro, C. E. A.; Santana, H. D.; Casado, C.; Coronas, J.; Zaia, D. A. M. *Astrobiology* **2011**, *11*, 409.
50. Titus, E.; Kalkar, A. K.; Gaikar, V. G. *Colloids Surf. A Physicochem. Eng. Asp.* **2003**, *223*, 55.
51. Klotz, I. M. *Science* **1958**, *128*, 815.
52. Kauzmann, W. *Adv. Protein Chem.* **1959**, *141*, 1.
53. Tsyganenko, A. A.; Storozheva, E. N.; Manoilova, O. V.; Lesage, T.; Daturi, M.; Lavalley, J. C. *Catal. Lett.* **2000**, *70*, 159.
54. Hunger, M. *Catalysis Reviews: Science and Engineering* **1997**, *39*, 345.
55. Daniell, W.; Schubert, U.; Glockler, R.; Meyer, A.; Noweck, K.; Knozinger, H. *Appl. Catal. A: Gen.* **2000**, *196*, 247.
56. Ivanov, Y.; Cheshkov, V.; Natova, M. *Polymer Composite Materials: Interface Phenomena and Processes*; Kluwer Academic Publishers: Dordrecht, 2001.
57. Nemethy, G.; Scheraga, H. A. *J. Phys. Chem.* **1962**, *66*, 1773.
58. Parbhakar, A.; Cuadros, J.; Sephton, M. A.; Dubbin, W.; Coles, B. J.; Weiss, D. *Colloid Surf. A* **2007**, *307*, 142.
59. Wang, Y.; Shang, Z.; Wu, T.; Fan, J.; Chen, X. *J. Mol. Catal. A: Chem.* **2006**, *253*, 212.
60. Zeidan, R. K.; Davis, M. E. *J. Catal.* **2007**, *247*, 379.